Article

Direct Measurement of the Hydrogen-Bonding Effect on the Intrinsic Redox Potentials of [4Fe–4S] Cubane Complexes

Xin Yang, Shuqiang Niu, Toshiko Ichiye, and Lai-Sheng Wang

J. Am. Chem. Soc., **2004**, 126 (48), 15790-15794• DOI: 10.1021/ja045709a • Publication Date (Web): 06 November 2004

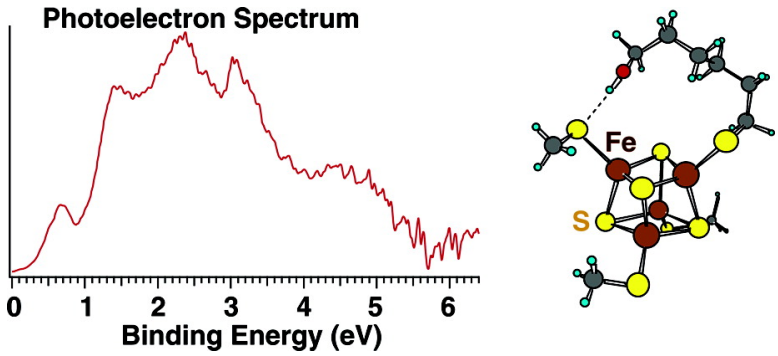

More About This Article

Additional resources and features associated with this article are available within the HTML version:

- Supporting Information
- Links to the 1 articles that cite this article, as of the time of this article download
- Access to high resolution figures
- Links to articles and content related to this article
- Copyright permission to reproduce figures and/or text from this article

View the Full Text HTML

J|A|C|S
ARTICLES
Published on Web 11/06/2004

Direct Measurement of the Hydrogen-Bonding Effect on the Intrinsic Redox Potentials of [4Fe−4S] Cubane Complexes

Xin Yang,[†] Shuqiang Niu,[‡] Toshiko Ichiye,[‡] and Lai-Sheng Wang*,[†]

Contribution from the Department of Physics, Washington State University, 2710 University Drive, Richland, Washington 99352, W. R. Wiley Environmental Molecular Sciences Laboratory, Pacific Northwest National Laboratory, P.O. Box 999, Richland, Washington 99352, and Department of Chemistry, Georgetown University, Washington, D.C. 20057-1227

Received July 16, 2004; E-mail: ls.wang@pnl.gov

Abstract: To probe how H-bonding effects the redox potential changes in Fe−S proteins, we produced and studied a series of gaseous cubane-type analogue complexes, $[Fe_4S_4(SEt)_3(SC_nH_{2n+1})]^{2-}$ and $[Fe_4S_4(SEt)_3(SC_nH_{2n}OH)]^{2-}$ (n = 4, 6, 11; Et = C_2H_5). Intrinsic redox potentials for the $[Fe_4S_4]^{2+/3+}$ redox couple involved in these complexes were measured by photoelectron spectroscopy. The oxidation energies from $[Fe_4S_4(SEt)_3(SC_nH_{2n}OH)]^{2-}$ to $[Fe_4S_4(SEt)_3(SC_nH_{2n}OH)]^{-}$ were determined directly from the photoelectron spectra to be ∼130 meV higher than those for the corresponding $[Fe_4S_4(SEt)_3(SC_nH_{2n+1})]^{2-}$ systems, because of the OH···S hydrogen bond in the former. Preliminary Monte Carlo and density functional calculations showed that the H-bonding takes place between the −OH group and the S on the terminal ligand in $[Fe_4S_4(SEt)_3(SC_6H_{12}OH)]^{2-}$. The current data provide a direct experimental measure of a net H-bonding effect on the redox potential of $[Fe_4S_4]$ clusters without the perturbation of other environmental effects.

Introduction

The [4Fe−4S] cluster is perhaps nature's most favorite agent for electron transfer and storage,[1] such as in ferredoxins (Fds),[2] high potential proteins (HiPIPs),[3] and the integral machineries of hydrogenases and nitrogenases.[4,5] In most cases, the iron and sulfide ligands are arranged in a slightly distorted cube with each iron additionally connected to a cysteinyl sulfur of the polypeptide chain. X-ray crystal structural data show that the [4Fe−4S] sites in different proteins exhibit similar Fe−S bond distances and bond angles for the bridging and terminal sulfur atoms.[2,6−13] However, the accessible oxidation states and the redox potentials of these [4Fe−4S] sites are enormously diverse.[14,15] With the structural similarity of the [4Fe−4S] core, major environmental factors have been suggested to contribute to the variations of the reduction potentials of Fe−S proteins, including H-bonding to the sulfide and terminal cysteine ligands, and electrostatic interactions with the Fe−S cluster from solvent and protein side-chain/backbone.[15−29] Among these factors, the H-bond between the amide N−H and the cysteine and bridging (S*) sulfide ligands of the cubane cluster may play important

[†] Washington State University and Pacific Northwest National Laboratory.
[‡] Georgetown University.

(1) Beinert, H.; Holm, R. H.; Münck, E. *Science* **1997**, *277*, 653−659.
(2) Dauter, Z.; Wilson, K. S.; Sieker, L. C.; Meyer, J.; Moulis, J. M. *Biochemistry* **1997**, *36*, 16065−16073.
(3) Kerfeld, C. A.; Salmeen, A. E.; Yeates, T. O. *Biochemistry* **1998**, *37*, 13911−13917.
(4) Peters, J. W.; Lanzilotta, W. N.; Lemon, B. J.; Seefeldt, L. C. *Science* **1998**, *282*, 1853−1858.
(5) Einsle, O.; Tezcan, F. A.; Andrade, S. L. A.; Schmid, B.; Yoshida, M.; Howard, J. B.; Rees, D. C. *Science* **2002**, *297*, 1696−1700.
(6) Carter, C. W., Jr.; Kraut, J.; Freer, S. T.; Alden, R. A. *J. Biol. Chem*. **1974**, *249*, 6339−6346.
(7) Carter, C. W., Jr. In *Iron−Sulfur Proteins*; Lovenberg, W., Ed.; Academic Press: New York, 1977; pp 157−204.
(8) Adman, E. T.; Sieker, L. C.; Jensen, L. H. *J. Biol. Chem*. **1973**, *248*, 3987−3996.
(9) Adman, E. T.; Sieker, L. C.; Jensen, L. H. *J. Biol. Chem*. **1976**, *251*, 3801−3806.
(10) Stout, G. H.; Turley, S.; Sieker, L. C.; Jensen, L. H. *Proc. Natl. Acad. Sci. U.S.A.* **1988**, *85*, 1020−1022.
(11) Stout, C. D. *J. Mol. Biol*. **1989**, *205*, 545−555.
(12) Fukuyama, K.; Nagahara, Y.; Tsukihara, T.; Katsube, Y. *J. Mol. Biol*. **1988**, *199*, 183−193.
(13) Fukuyama, K.; Nagahara, Y.; Tsukihara, T.; Katsube, Y. *J. Mol. Biol*. **1989**, *210*, 383−398.
(14) Cammack, R. Iron−Sulfur Cluster in Enzymes: Themes and Variations. In *Iron−Sulfur Proteins*; Cammack, R., Ed.; Academic Press: San Diego, CA, 1992; pp 281−322.
(15) Stephens, P. J.; Jollie, D. R.; Warshel, A. *Chem. Rev*. **1996**, *96*, 2491−2513.
(16) Adman, E. T.; Watenpaugh, K. D.; Jensen, L. H. *Proc. Natl. Acad. Sci. U.S.A.* **1975**, *72*, 4854−4858.
(17) Kasner, R. J.; Yang, W. *J. Am. Chem. Soc*. **1977**, *99*, 4351−4355.
(18) Sheridan, R. P.; Allen, L. C.; Carter, C. W., Jr. *J. Biol. Chem*. **1981**, *256*, 5052−5057.
(19) Backes, G.; Mino, Y.; Loehr, T. M.; Meyer, T. E.; Cusanovich, M. A.; Sweeney, W. V.; Adman, E. T.; Sanders-Loehr, J. *J. Am. Chem. Soc.* **1991**, *113*, 2055−2064.
(20) Kodaka, M.; Tomohiro, T.; Okuno, H. *J. Phys. Chem*. **1991**, *95*, 6741−6744.
(21) Langen, R.; Jensen, G. M.; Jacob, U.; Stephens, P. J.; Warshel, A. *J. Biol. Chem*. **1992**, *267*, 25625−25627.
(22) Pickett, C. J.; Ryder, K. S. *J. Chem. Soc., Dalton Trans.* **1994**, 2181−2189.
(23) Banci, L.; Bertini, I.; Savellini, G. G.; Luchinat, C. *Inorg. Chem*. **1996**, *35*, 4248−4253.
(24) Cowan, J. A.; Liu, S. M. *Adv. Inorg. Chem*. **1997**, *45*, 313−350.
(25) Chen, K.; Tilley, G. J.; Sridhar, V.; Prasad, G. S.; Stout, C. D.; Armstrong, F. A.; Burgess, B. K. *J. Biol. Chem*. **1999**, *274*, 36479−36487.
(26) Babini, E.; Borsari, M.; Capozzi, F.; Eltis, L. D.; Luchinat, C. *J. Biol. Inorg. Chem*. **1999**, *4*, 692−700.
(27) Zhou, C.; Raebiger, J. W.; Segal, B. M.; Holm, R. H. *Inorg. Chim. Acta* **2000**, *300−302*, 892−902.
(28) Beck, B. W.; Xie, Q.; Ichiye, T. *Biophys. J*. **2001**, *81*, 601−613.
(29) Glaser, T.; Bertini, I.; Moura, J. J. G.; Hedman, B.; Hodgson, K. O.; Solomon, E. I. *J. Am. Chem. Soc*. **2001**, *123*, 4859−4860.

10.1021/ja045709a CCC: $27.50

roles. For instance, eight NH···S (S* and Cys S) H-bonds were identified in *Pa*Fd, while five such H-bonds were found in the case of *Cv*HiPIP. The larger number of H-bonds in Fd than in HiPIP presumably favors a lower oxidation level in Fd's.[7,16] However, due to the extreme complexity of the protein environment, it is difficult to build a simple correlation between the cluster−protein H-bonding and the redox potential.[15] Numerous efforts had been made to investigate the protein environment of the Fe−S cluster,[15−29] but the net H-bonding effect on the redox potential of Fe−S protein remains uncertain.[30]

Gas-phase photodetachment photoelectron spectroscopy is a powerful experimental technique to study the electronic structure and chemical bonding of isolated molecules without perturbation of the solvents, the crystal field, or the protein environment, yielding intrinsic properties of the Fe−S clusters and providing the basis for elucidating the complex cluster−protein interactions. Photodetachment, involving removal of an electron from an anion ($AB^{n-} \rightarrow AB^{(n-1)} + e^-$), is an oxidation process. The measured adiabatic electron detachment energy (ADE) reflects the energy difference between the oxidized and reduced species in the gas phase, providing the intrinsic redox potential.[31] We have developed an experimental technique, which couples an electrospray ionization source with a magnetic-bottle photoelectron spectrometer.[32] Electrospray is a versatile technique, allowing ionic species in solution samples to be transported into the gas phase. Our recent work has shown that photoelectron spectroscopy plus electrospray is an ideal technique for investigating multiply charged anions in the gas-phase,[33] as well as anionic metal-complexes commonly present in solution.[31,34,35] Using this technique, we have reported systematic photoelectron spectroscopic and theoretical studies on a series of [1Fe] to [4Fe−4S] complex anions as the analogues of the active centers of different Fe−S proteins.[36−40]

In the current work, we want to address how a single H-bond influences the redox potential of a [4Fe−4S] cubane complex. We report a photoelectron spectroscopic study on a series of gaseous doubly charged cubane complexes, $[Fe_4S_4(SEt)_3(SC_nH_{2n+1})]^{2-}$ and $[Fe_4S_4(SEt)_3(SC_nH_{2n}OH)]^{2-}$ (n = 4, 6, 11; Et = C_2H_5). These complexes can be viewed as the analogue of the active site of [4Fe−4S] proteins. The $-SC_nH_{2n}OH$-coordinated complexes were expected to form an intramolecular H-bond between the hydroxyl group and the cubane sulfur, while the $-SC_nH_{2n+1}$-coordinated complexes were used as non-H-bonding references. Theoretical calculations were used to understand the H-bonding conformation of $[Fe_4S_4(SEt)_3(SC_nH_{2n}OH)]^{2-}$. The measured oxidation energies for $[Fe_4S_4(SEt)_3(SC_nH_{2n}OH)]^{2-}$ are 130 meV higher than those of the corresponding $[Fe_4S_4(SEt)_3(SC_nH_{2n+1})]^{2-}$, revealing that a single OH···S hydrogen bond can change the redox potential of a [4Fe−4S] cubane by as much as 130 mV.

Materials and Methods

Photoelectron Spectroscopy. The experiment was carried out using an experimental apparatus equipped with a magnetic-bottle photoelectron analyzer and an electrospray source. Details of the experimental method have been given elsewhere.[32] Briefly, the sample solutions were prepared by dissolving $(Bu_4N)_2[Fe_4S_4(SEt)_4]$ and $C_nH_{2n+1}SH$ or $HSC_nH_{2n}OH$ (n = 4, 6, 11) in O_2-free acetonitrile at 4:1 molar ratios. The $[Fe_4S_4(SEt)_3(SC_nH_{2n+1})]^{2-}$ and $[Fe_4S_4(SEt)_3(SC_nH_{2n}OH)]^{2-}$ (n = 4, 6, 11) complexes were produced by terminal ligand substitution reactions[41] and were introduced into the gas phase by electrospray. Anions generated from the electrospray source were guided into a quadruple ion-trap, where ions were accumulated for 0.1 s before being pulsed into the extraction zone of a time-of-flight mass spectrometer. The ion trap was kept at room temperature. Therefore, the internal temperatures of the anions were also expected to be around room temperature.

During the photoelectron spectroscopy experiment, the anions of interest were mass-selected and decelerated before being intercepted by a probe laser beam in the photodetachment zone of the magnetic-bottle photoelectron analyzer. In the current study, we employed three detachment photon energies, 355 nm (3.496 eV), and 266 nm (4.661 eV) from a Nd:YAG laser, and 193 nm (6.424 eV) from an excimer laser. Photoelectrons were collected at nearly 100% efficiency by the magnetic bottle and analyzed in a 4-m long electron flight tube. Photoelectron time-of-flight spectra were collected and then converted to kinetic energy spectra, calibrated by the known spectra of I^- and O^-. The electron binding energy spectra presented here were obtained by subtracting the kinetic energy spectra from the detachment photon energies (EB = $h\nu$ − KE). The electron kinetic energy resolution (ΔKE/KE) was about 2%, that is, ∼10 meV for 0.5 eV electrons, as measured from the spectrum of I^- at 355 nm.

Theoretical Methods. Monte Carlo (MC) simulations followed by the molecular mechanic (MM) minimization method was employed for searching the conformations of $[Fe_4S_4(SCH_3)_3(SR)]^{2-}$ (R = $-C_6H_{13}$ and $-C_6H_{12}OH$) using the HyperChem molecular modeling package.[42] We used the simpler $-SCH_3$ ligand in all of the calculations, instead of the more complex −SEt ligand, which does not significantly change the structures and electronic properties of the complexes. The MM+ force field and parameters were utilized for MC and MM calculations. The MC simulations and MM calculations only involve the SC_6H_{13}, $SC_6H_{12}OH$, and H-bonded S of the $-SCH_3$ and sulfide ligands of $[Fe_4S_4(SCH_3)_3(SR)]^{2-}$, in which the geometries are constrained at the possible H-bonded structures and the cubane core is constrained to the DFT optimized structure of $[Fe_4S_4(SCH_3)_4]^{2-}$. The MC simulations were run 20 000 steps around each possible conformation structure at 1000 K.

The broken-symmetry (BS) DFT method,[43,44] specifically with the Becke's three-parameter hybrid exchange functional,[45−47] the B3LYP correlation functional,[48] and the 6-31G**/6-311G** basis sets,[49−51] were

(30) Reference 26 reported that one NH···S H-bond contributes ∼100 mV to the reduction potential of metalloprotein by comparing the *Chromatium vinosum* HiPIP and its S79P variant. However, the possibility of the main-chain orientation change induced by the H-bond cannot be ruled out in this work, which also affects the reduction potential (ref 28).

(31) Wang, X. B.; Wang. L. S. *J. Chem. Phys*. **2000**, *112*, 6959−6962.
(32) Wang, L. S.; Ding, C. F.; Wang, X. B.; Barlow, S. E. *Rev. Sci. Instrum*. **1999**, *70*, 1957−1966.
(33) Wang, L. S.; Wang, X. B. *J. Phys. Chem. A* **2000**, *104*, 1978−1990.
(34) Wang, X. B.; Wang, L. S. *J. Am. Chem. Soc*. **2000**, *122*, 2339−2345.
(35) Wang, X. B.; Wang, L. S. *J. Am. Chem. Soc*. **2000**, *122*, 2096−2100.
(36) Yang, X.; Wang, X. B.; Fu, Y. J.; Wang, L. S. *J. Phys. Chem. A* **2003**, *107*, 1703−1709.
(37) Niu, S. Q.; Wang, X. B.; Nichols, J. A.; Wang, L. S.; Ichiye, T. *J. Phys. Chem. A* **2003**, *107*, 2898−2907.
(38) Yang, X.; Razavet, M.; Wang, X. B.; Pichett, C. J.; Wang, L. S. *J. Phys. Chem. A* **2003**, *107*, 4612−4618.
(39) Yang, X.; Wang, X. B.; Niu, S. Q.; Pickett, C. J.; Ichiye, T.; Wang, L. S. *Phys. Rev. Lett.* **2002**, *89*, 16340-1−4.
(40) Wang, X. B.; Niu, S. Q.; Yang, X.; Ibrahim, S. K.; Pickett, C. J.; Ichiye, T.; Wang, L. S. *J. Am. Chem. Soc*. **2003**, *125*, 14072−14081.

(41) Que, L.; Bobrik, M. A.; Ibers, J. A.; Holm, R. H. *J. Am. Chem. Soc*. **1974**, *96*, 4168−4178. Statistically, it is possible to form $-OC_nH_{2n}SH$ coordinated isomer in the ligand substitution reaction. However, the acidity of −SH is much stronger than the −OH group, making the possibility to form the $-OC_nH_{2n}SH$ substituted complex very small.

(42) *HyperChem Professional 7.0*; Hypercube, Inc.: 115 NW 4th Sreen, Gainesville, FL 32601.
(43) Parr, R. G.; Yang, W. *Density-Functional Theory of Atoms and Molecules*; Oxford University Press: Oxford, 1989.
(44) Noodleman, L.; Peng, C. Y.; Case, D. A.; Mouesca, J.-M. *Coord. Chem. Rev*. **1995**, *144*, 199−241.
(45) Becke, A. D. *Phys. Rev. A* **1988**, *38*, 3098−3100.
(46) Becke, A. D. *J. Chem. Phys.* **1993**, *98*, 1372−1377.
(47) Becke, A. D. *J. Chem. Phys.* **1993**, *98*, 5648−5652.
(48) Lee, C.; Yang, W.; Parr, R. G. *Phys. Rev. B* **1988**, *37*, 785−789.

utilized for the geometry optimizations and electronic structure calculations. The calculated energies were refined at the B3LYP/6-31-(++)$_S$G**//B3LYP/6-31G** level, where sp-type diffuse functions were added to the 6-31G** basis set of the sulfur and oxygen atoms.[49−54] The ADE of $[Fe_4S_4(SCH_3)_3(SR)]^{2-}$ was calculated as the total energy difference between the ground states of $[Fe_4S_4(SCH_3)_3(SR)]^{2-}$ and $[Fe_4S_4(SCH_3)_3(SR)]^{-}$; the VDE was calculated as the energy difference between the ground state of $[Fe_4S_4(SCH_3)_3(SR)]^{2-}$ and the energy of $[Fe_4S_4(SCH_3)_3(SR)]^{-}$ at the geometry of $[Fe_4S_4(SCH_3)_3(SR)]^{2-}$. Because the spin projection corrections for BS DFT energies of the reduced and oxidized sites of HiPIP analogues tend to cancel each other when computing the oxidation energies or relative energies,[55] spin-coupling effects on BS-DFT calculations were neglected in this work. All calculations were performed using the NWChem program package.[56]

Results and Discussion

Photoelectron Spectra and Electron Binding Energies. Photoelectron spectra of all six cubane complexes were taken at three photon energies: 355, 266, and 193 nm. We observed that the terminal ligand substitution has little effect on the overall spectral patterns, which are almost identical to those of $[Fe_4S_4(SEt)_4]^{2-}$.[40] Only the spectra of $[Fe_4S_4(SEt)_3(SC_6H_{12}OH)]^{2-}$ are shown here (Figure 1). A well-defined threshold feature *X* was observed in the photoelectron spectra of all of the cubane complexes. A second band *A*, well separated from the *X* band, was overlapped with high binding energy features. The higher binding energy part of the spectra appeared to be broad and almost continuous. In the lower photon energy spectra, high binding energy features disappeared as a direct consequence of the repulsive coulomb barrier universally present in multiply charged anions.[33]

Despite the overall similarities of the spectral patterns among the six cubane complexes, their electron binding energies were observed to depend on the type of substituents. To display the spectral shift, we show in Figure 2 the 355 nm spectra of all six cubane complexes. The spectra in red show that the electron binding energies of $[Fe_4S_4(SEt)_3(SC_nH_{2n+1})]^{2-}$ increases steadily with the chain length of the substituted ligand from $n = 4$ to 11. The same trend was observed for the $[Fe_4S_4(SEt)_3(SC_nH_{2n}OH)]^{2-}$ series (in black). However, the binding energies of the $-SC_nH_{2n}OH$-substituted complexes were observed to be systematically higher than those of the $-SC_nH_{2n+1}$-substituted complexes with the same chain length. The ADE and VDE (vertical detachment energy) of the threshold peak are given in Table 1, where the oxidation reorganization energies (λ_{oxd}) are also given.[31,57]

Terminal Ligand Effect on the ADEs. The terminal ligand effects on the electron binding energies have been well documented in our prior studies. In a series of $[Fe_4S_4L_4]^{2-}$ cubane complexes, we have shown that the [4Fe−4S] core is a robust unit and its overall electronic structure does not change too much upon the terminal ligand substitution.[40] Yet its intrinsic redox potential, as measured by the ADE of the $[Fe_4S_4L_4]^{2-}$ complexes from photoelectron spectroscopy, is strongly de-

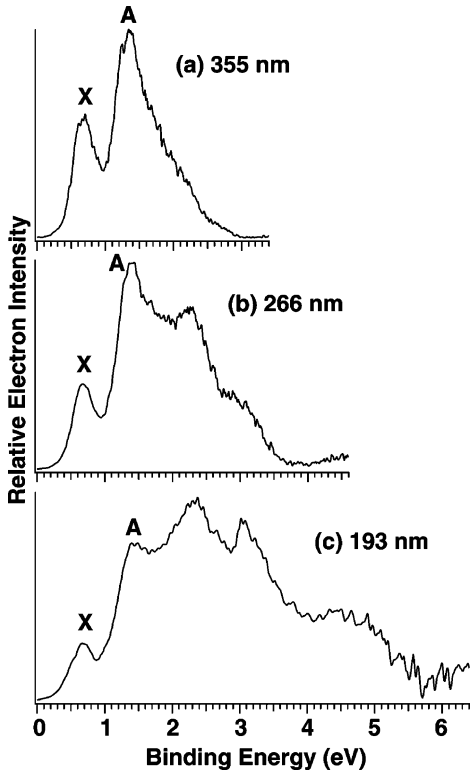

Figure 1. Photoelectron spectra of $[Fe_4S_4(SEt)_3(SC_6H_{12}OH)]^{2-}$ at (a) 355 nm (3.496 eV), (b) 266 nm (4.661 eV), and (c) 193 nm (6.424 eV).

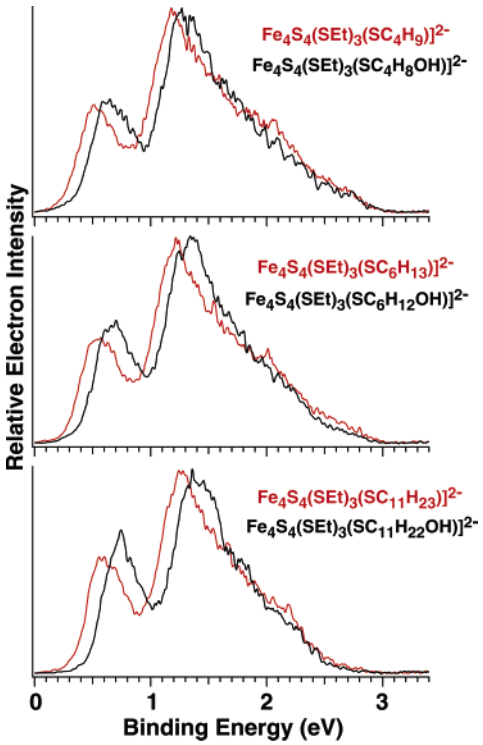

Figure 2. Photoelectron spectra of $[Fe_4S_4(SEt)_3(SC_nH_{2n+1})]^{2-}$ (red curves) and $[Fe_4S_4(SEt)_3(SC_nH_{2n}OH)]^{2-}$ (black curves) ($n = 4$, 6, 11) at 355 nm.

(49) Rassolov, V.; Pople, J. A.; Ratner, M.; Windus, T. L. *J. Chem. Phys.* **1998**, *109*, 1223−1229.
(50) Francl, M. M.; Petro, W. J.; Hehre, W. J.; Binkley, J. S.; Gordon, M. S.; DeFrees, D. J.; Pople, J. A. *J. Chem. Phys.* **1982**, *77*, 3654−3665.
(51) Hariharan, P. C.; Pople, J. A. *Theor. Chim. Acta* **1973**, *28*, 213−222.
(52) Clark, T.; Chandrasekhar, J.; Schleyer, P. v. R. *J. Comput. Chem.* **1983**, *4*, 294−301.
(53) Krishnam, R.; Binkley, J. S.; Seeger, R.; Pople, J. A. *J. Chem. Phys.* **1980**, *72*, 650−654.
(54) Gill, P. M. W.; Johnson, B. G.; Pople J. A.; Frisch, M. J. *Chem. Phys. Lett.* **1992**, *97*, 499−505.
(55) Torres, R. A.; Lovell, T.; Noodleman, L.; Case, D. A. *J. Am. Chem. Soc.* **2003**, *125*, 1923−1936.
(56) High Performance Computational Chemistry Group. *NWChem, A Computational Chemistry Package for Parallel Computers, Version 4.5*; Pacific Northwest National Laboratory: Richland, WA 99352, 2003.
(57) Amashukeli, X.; Winkler, J. R.; Gray, H. B.; Gruhn, N. E.; Lichtenberger, D. L. *J. Phys. Chem. A.* **2002**, *106*, 7593−7598.

Table 1. Experimental Adiabatic Detachment Energies (ADE), Vertical Detachment Energies (VDE),[a] and Oxidation Reorganization Energies (λ_{oxd}) for $[Fe_4S_4(SEt)_3(SC_nH_{2n+1})]^{2-}$ and $[Fe_4S_4(SEt)_3(SC_nH_{2n}OH)]^{2-}$ ($n = 4, 6, 11$) (All Energies Are in eV)

$[Fe_4S_4(SEt)_3(SR)]^{2-}$	ADE	VDE	ΔADE[b]	λ_{oxd}[c]
$[Fe_4S_4(SEt)_3(SC_4H_9)]^{2-}$	0.31	0.53	0.13	0.22
$[Fe_4S_4(SEt)_3(SC_4H_8OH)]^{2-}$	0.44	0.66		0.22
$[Fe_4S_4(SEt)_3(SC_6H_{13})]^{2-}$	0.34	0.57	0.12	0.23
$[Fe_4S_4(SEt)_3(SC_6H_{12}OH)]^{2-}$	0.46	0.68		0.22
$[Fe_4S_4(SEt)_3(SC_{11}H_{23})]^{2-}$	0.41	0.63	0.13	0.22
$[Fe_4S_4(SEt)_3(SC_{11}H_{22}OH)]^{2-}$	0.54	0.76		0.22

[a] Due to the lack of vibrational resolution, the ADEs were measured by drawing a straight line along the leading edge of the threshold band and then adding a constant to the intersection with the binding energy axis to take into account the instrumental resolution at the given energy range. This procedure, although approximate, did give consistent data for spectra taken at different photon energies. The VDE was measured straightforwardly from the peak maximum. The estimated uncertainty for the ADEs and VDEs was ± 0.06 eV. [b] The ΔADE represents the ADE difference between $[Fe_4S_4(SEt)_3(SC_nH_{2n}OH)]^{2-}$ and $[Fe_4S_4(SEt)_3(SC_nH_{2n+1})]^{2-}$. [c] These values were defined as (VDE − ADE). See ref 31.

pendent on the electron-donating or -withdrawing ability of the terminal ligands. Strong electron donor ligands, such as $-SR$, raise the energy of the highest occupied molecular orbital (HOMO) of $[Fe_4S_4L_4]^{2-}$, yielding a lower ADE, whereas strong electron-withdrawing ligands, such as the halogens, lower the energy of the HOMO of $[Fe_4S_4L_4]^{2-}$ and give relatively high ADE. The electron-withdrawing ability of the $-SC_nH_{2n+1}$ ligands increases with the alkyl chain, as can be seen from the increasing electron affinities of SC_nH_{2n+1} (1.867, 1.953, 2.00, 2.03, 2.09 eV for $n = 1-5$, respectively).[58,59] This explains the ADE increases in the $[Fe_4S_4(SEt)_3(SC_nH_{2n+1})]^{2-}$ series, because the ability of $-SC_nH_{2n+1}$ to stabilize the negative charge becomes greater with increasing alkyl chain length.[59]

Intramolecular H-Bonding: $[Fe_4S_4(SEt)_3(SC_nH_{2n+1})]^{2-}$ versus $[Fe_4S_4(SEt)_3(SC_nH_{2n}OH)]^{2-}$. Because of the induction effect of the $-OH$ group, an increase in ADE for $[Fe_4S_4(SEt)_3(SC_nH_{2n}OH)]^{2-}$ relative to $[Fe_4S_4(SEt)_3(SC_nH_{2n+1})]^{2-}$ was expected. Because the induction effect decreases rapidly with the chain length, it was also expected that the magnitude of the ADE increase of $[Fe_4S_4(SEt)_3(SC_nH_{2n}OH)]^{2-}$ relative to $[Fe_4S_4(SEt)_3(SC_nH_{2n+1})]^{2-}$ should also decrease with increasing chain length. However, this was not the case, as can be seen from Table 1, where we listed the ADE increase of $[Fe_4S_4(SEt)_3(SC_nH_{2n}OH)]^{2-}$ relative to $[Fe_4S_4(SEt)_3(SC_nH_{2n+1})]^{2-}$ as ΔADE. Surprisingly, the ΔADE is identical ($\sim$130 meV) within our experimental uncertainty, regardless of the substituent chain lengths. Therefore, the induction effect of the hydroxyl group is not sufficient to explain our experimental observation.

The only explanation consistent with our experimental results is that somehow the $-OH$ group is directly interacting with the cubane core. The hydroxyl group is a well-known H-bonding donor. Ab initio quantum calculations have shown that the Fe-ligated sulfurs are good H-bond acceptors.[60] It is reasonable to believe that in $[Fe_4S_4(SEt)_3(SC_nH_{2n}OH)]^{2-}$ the $-SC_nH_{2n}OH$ ligand may fold back to the cubane and form a strong intramolecular H-bond between the $-OH$ and S either from the terminal ligand or the bridging inorganic sulfur within the cubane core. The alkyl chain is relatively flexible, and the strong H-bonding can compensate for any energy cost for the folding. Electronically this OH···S H-bond is expected to stabilize the negative charges on the cubane, thus increasing the oxidation energy of the cubane complexes. Because the H-bonding strength for all three $[Fe_4S_4(SEt)_3(SC_nH_{2n}OH)]^{2-}$ ($n = 4, 6, 11$) complexes should be the same, the increment of the ADE relative to the respective $[Fe_4S_4(SEt)_3(SC_nH_{2n+1})]^{2-}$ complexes, in which there is no H-bonding, is also expected to be the same, in exact agreement with our experimental observation. Here, the $[Fe_4S_4(SEt)_3(SC_nH_{2n+1})]^{2-}$ species serve as non-H-bonding references; thus the ΔADE we measured corresponds to the net H-bonding effect on the oxidation energy.

Table 2. B3LYP/6-31(++)$_S$G** Adiabatic Detachment Energies (ADE) and Vertical Detachment Energies (VDE) (in eV) for $[Fe_4S_4(SCH_3)_3(SR)]^{2-}$ (R = $-CH_3$, $-C_6H_{13}$, and $-C_6H_{12}OH$)

	ADE		VDE	
$[Fe_4S_4(SCH_3)_3(SR)]^{2-}$	calcd	exptl	calcd	exptl
$[Fe_4S_4(SCH_3)_4]^{2-}$	0.16	0.29	0.46	0.52
$[Fe_4S_4(SCH_3)_3(SC_6H_{13})]^{2-}$	0.17	0.34	0.55	0.56
$[Fe_4S_4(SCH_3)_3(SC_6H_{12}OH)]^{2-}$ (non-H-bond)	0.22		0.59	
$[Fe_4S_4(SCH_3)_3(SC_6H_{12}OH)]^{2-}$ (H-bond)	0.31	0.46	0.67	0.68

Preliminary Theoretical Results and Confirmation of the Intramolecular H-Bonding. To confirm the intramolecular H-bonding in the $-SC_nH_{2n}OH$-substituted cubane complexes, we carried out preliminary theoretical calculations using $[Fe_4S_4(SCH_3)_3(SC_6H_{12}OH)]^{2-}$ as a model. Two of the most important conformational structures of this complex, one with and one without a H-bond, were isolated by MC simulations, followed by MM and DFT optimizations. The results are compared with the optimized conformation of $[Fe_4S_4(SCH_3)_3(SC_6H_{13})]^{2-}$ in Figure 3. For $[Fe_4S_4(SCH_3)_3(SC_6H_{13})]^{2-}$, the long-chain thiol ligand $-SC_6H_{13}$ assumes a quasi-linear conformation and points away from the cubane core (Figure 3c). For $[Fe_4S_4(SCH_3)_3(SC_6H_{12}OH)]^{2-}$, both the H-bonding (Figure 3a) and the non-H-bonding (Figure 3b) conformations are energy minima, but the former is more stable by 3.1 kcal/mol. The most favorable H-bonding location is the diagonal terminal ligand sulfur.[61] The distance between oxygen and sulfur of OH···S is 3.3 Å, which is compatible to the NH···S H-bonds in Fds and HiPIP ($\sim$3.5 Å N−S distance).[19] The H-bonding interaction between the $-OH$ group and the $-SEt$ ligand stabilizes the high-lying occupied molecular orbitals on the [2Fe−2S] layer by its side, resulting in a shorter Fe−Fe distance by 0.05 Å ($Fe_{oxd}-Fe_{oxd}$ in Figure 3a).

Oxidation energies for $[Fe_4S_4(SCH_3)_3(SC_6H_{13})]^{2-}$ and the two conformations of $[Fe_4S_4(SCH_3)_3(SC_6H_{12}OH)]^{2-}$ were also calculated (Table 2). Note that the calculated ADEs are low relative to the experimental ADEs, whereas the calculated VDEs are in much better agreement with the experimental VDEs.[62] In comparison to $[Fe_4S_4(SCH_3)_4]^{2-}$, the slightly weaker electron donor ligand, $-SC_6H_{13}$, only induces a very small increase ($\sim$0.01 eV) in the oxidation energy (ADE), consistent with the

(58) Rienstra-Kiracofe, J. C.; Tschumper, G. S.; Schaefer, H. F., III; Nandi, S.; Ellison, G. B. *Chem. Rev.* **2002**, *102*, 231−282.
(59) Janousek, B. K.; Reed, K. J.; Brauman, J. I. *J. Am. Chem. Soc.* **1980**, *102*, 3125−3129.
(60) Koerner, J. B.; Ichiye, T. *J. Phys. Chem. B* **2000**, *104*, 2424−2431.

(61) The MD simulations suggested that the thiolate H-bond is more favorable over the sulfide H-bond. DFT calculations show that H-bonding to the sulfide only brings a stabilization of 1.7 kcal/mol relative to the non-H-bonded conformation. We plan to publish more details in a future theoretical paper.
(62) The large errors in ADEs were due to the fact that the ADE calculations involved the total energies at the optimized structures of both the dianions and the final state singly charged anions, whereas the VDEs only involved the energy difference between the dianions and the singly charged anions both at the optimized structure of the initial dianions.

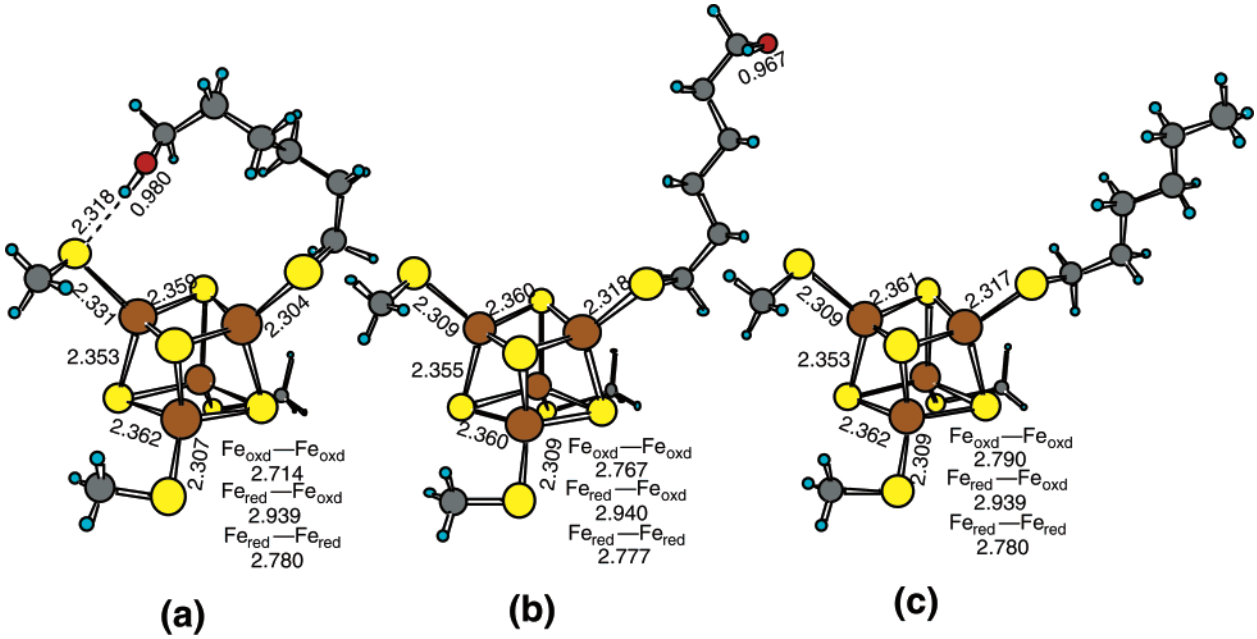

Figure 3. B3LYP/6-31G** optimized structures of (a) the H-bonding conformation of $[Fe_4S_4(SCH_3)_3(SC_6H_{12}OH)]^{2-}$, (b) the non-H-bonding conformation of $[Fe_4S_4(SCH_3)_3(SC_6H_{12}OH)]^{2-}$, and (c) $[Fe_4S_4(SCH_3)_3(SC_6H_{13})]^{2-}$. The Fe−Fe distances within the cubane are also given (Fe_{oxd} refers the top Fe_2S_2 layer, and Fe_{red} refers to the bottom Fe_2S_2 layer). All bond lengths shown are given in angstroms.

experimental results, which showed an ADE increase of about 0.05 eV. For the non-H-bonding conformation of the $-SC_6H_{12}$-OH-substituted cubane, an ADE of 0.22 eV was obtained from our calculations, which was 0.05 eV higher than the $-SC_6H_{13}$-substituted cubane. This 0.05 eV increase can be viewed to be due to the induction effect of the −OH group. Most importantly, the ADE of the H-bonding conformation of $[Fe_4S_4(SCH_3)_3(SC_6H_{12}OH)]^{2-}$ was calculated to be 0.31 eV, which is 0.14 eV higher than that of $[Fe_4S_4(SCH_3)_3(SC_6H_{13})]^{2-}$, in excellent agreement with the experimental measurement. The VDEs of the respective cubane complexes were also calculated, and they agree in general much better with the experimental data, probably due to favorable cancellation of errors because no geometry changes were involved when the VDEs were calculated.

The current results should be relevant to the influence of redox potentials due to H-bonding in the protein environment. The amide group, ubiquitous in proteins, is a H-bonding donor similar to the hydroxyl group, so one NH···S hydrogen bond should contribute similarly to the redox potentials of Fe−S proteins. In *Cv*HIPIP, the main-chain amide group between residue Ala78 and Ser79 is in close proximity to the [4F−4S] cubane core and forms a H-bond with the S atom of Cys77, which is one of the four cluster ligands. When Ser79 is replaced with proline, so that there is no amide H-bonding to Cys77, the reduction potential of the S79P variant is lowered by 104 mV.[26] Despite the vastly different environment between the protein and the model complexes, the effect due to a single amide H-bond change to the terminal S in the cubane in *Cv*HiPIP has a magnitude similar to that of the H-bond effect in the current analogue complexes.

Conclusions

We investigated the effect of a single H-bond on the redox potentials of a series of analogue cubane complexes, $[Fe_4S_4(SEt)_3(SC_nH_{2n}OH)]^{2-}$ ($n = 4, 6, 11$), using photoelectron spectroscopy and theoretical calculations. Photoelectron spectra showed the ADEs of $[Fe_4S_4(SEt)_3(SC_nH_{2n}OH)]^{2-}$ ($n = 4, 6, 11$) are higher than those of the corresponding $[Fe_4S_4(SEt)_3(SC_nH_{2n+1})]^{2-}$ systems by a similar amount (∼130 meV) due to the intramolecular H-bond between the OH group in $SC_nH_{2n}OH$ and the S coordinated to the cubane. Monte Carlo simulations and DFT calculations revealed the stability of this OH···S bonding conformation and showed that the most favored H-bonding site is between the hydroxyl group and the diagonal terminal ligand sulfur. The current study provides a direct experimental measurement of the net effect of a H-bond on the oxidation potential of analogue complexes with a $[Fe_4S_4]^{2+}$ cubane core, without perturbation of other environmental effects: one OH··· S hydrogen bond to the terminal ligand S raises the oxidation potential by ∼130 mV.

Acknowledgment. Support by the National Institutes of Health (GM-63555 to L.-S.W. and GM-45303 to T.I.) is gratefully acknowledged. The experimental work and some of the calculations (using the Molecular Science Computing Facility) were performed at the W. R. Wiley Environmental Molecular Sciences Laboratory, a national scientific user facility sponsored by DOE's Office of Biological and Environmental Research and located at Pacific Northwest National Laboratory, which is operated for DOE by Battelle.

JA045709A